

## Article

# Co-Combustion Studies of Low-Rank Coal and Refuse-Derived Fuel: Performance and Reaction Kinetics

Mudassar Azam <sup>1,2,\*</sup>, Asma Ashraf <sup>2,3</sup>, Saman Setoodeh Jahromy <sup>1</sup>, Sajjad Miran <sup>4</sup>, Nadeem Raza <sup>5</sup>, Florian Wesenauer <sup>1</sup>, Christian Jordan <sup>1</sup>, Michael Harasek <sup>1</sup> and Franz Winter <sup>1</sup>

<sup>1</sup> Institute of Chemical, Environmental and Bioscience Engineering, Vienna University of Technology (TU WIEN), Getreidemarkt 9, 1060 Vienna, Austria; saman.setoodeh.jahromy@tuwien.ac.at (S.S.J.); florian.wesenauer@tuwien.ac.at (F.W.); christian.jordan@tuwien.ac.at (C.J.); michael.harasek@tuwien.ac.at (M.H.); franz.winter@tuwien.ac.at (F.W.)

<sup>2</sup> Institute of Chemical Engineering & Technology (ICET), University of the Punjab, Lahore 54590, Pakistan; aasma.ashraf@hotmail.com

<sup>3</sup> Sharif College of Engineering & Technology, University of Engineering and Technology (UET), Lahore 39161, Pakistan

<sup>4</sup> Department of Mechanical Engineering, University of Gujrat, Gujrat 50700, Pakistan; sajjad.miran@uog.edu.pk

<sup>5</sup> Department of Chemistry, Emerson University Multan, Multan 60000, Pakistan; nadeemr8@hotmail.com

\* Correspondence: mudassar.azam@tuwien.ac.at or mudassar.icet@pu.edu.pk



**Citation:** Azam, M.; Ashraf, A.; Setoodeh Jahromy, S.; Miran, S.; Raza, N.; Wesenauer, F.; Jordan, C.; Harasek, M.; Winter, F. Co-Combustion Studies of Low-Rank Coal and Refuse-Derived Fuel: Performance and Reaction Kinetics. *Energies* **2021**, *14*, 3796. <https://doi.org/10.3390/en14133796>

Academic Editors: Wojciech Nowak, Jaroslaw Krzywanski and Karol Szteklar

Received: 3 May 2021

Accepted: 18 June 2021

Published: 24 June 2021

**Publisher's Note:** MDPI stays neutral with regard to jurisdictional claims in published maps and institutional affiliations.



**Copyright:** © 2021 by the authors. Licensee MDPI, Basel, Switzerland. This article is an open access article distributed under the terms and conditions of the Creative Commons Attribution (CC BY) license (<https://creativecommons.org/licenses/by/4.0/>).

**Abstract:** In connection to present energy demand and waste management crisis in Pakistan, refuse-derived fuel (RDF) is gaining importance as a potential co-fuel for existing coal fired power plants. This research focuses on the co-combustion of low-quality local coal with RDF as a mean to reduce environmental issues in terms of waste management strategy. The combustion characteristics and kinetics of coal, RDF, and their blends were experimentally investigated in a micro-thermal gravimetric analyzer at four heating rates of 10, 20, 30, and 40 °C/min to ramp the temperature from 25 °C to 1000 °C. The mass percentages of RDF in the coal blends were 10%, 20%, 30%, and 40%, respectively. The results show that as the RDF in blends increases, the reactivity of the blends increases, resulting in lower ignition temperatures and a shift in peak and burnout temperatures to a lower temperature zone. This indicates that there was certain interaction during the combustion process of coal and RDF. The activation energies of the samples were calculated using kinetic analysis based on Kissinger–Akahira–Sunose (KAS) and Flynn–Wall–Ozawa (FWO), isoconversional methods. Both of the methods have produced closer results with average activation energy between 95–121 kJ/mol. With a 30% refuse-derived fuel proportion, the average activation energy of blends hit a minimum value of 95 kJ/mol by KAS method and 103 kJ/mol by FWO method.

**Keywords:** waste to energy; refuse-derived fuel; co-combustion; kinetics; low-rank coal

## 1. Introduction

Global warming and anthropogenic emission of CO<sub>2</sub> are crucial issues and have achieved great attention due to their critical impact on human society and ecosystem [1]. Due to the rapid increase in population, urbanization, and industrialization, the earth is facing serious environmental challenges. These are mainly linked to: (a) management of the enormous amount of generated municipal solid waste (MSW), and (b) extensive utilization of fossil fuels, especially coal, as the prime energy source to meet the ever-increasing demand for energy. Worldwide, the generation of MSW in 2016 was 2.01 billion tons, which is expected to increase to 3.4 billion tons by 2050 [2]. Due to lack of engineered landfills and other environmentally friendly treatment facilities, most of the world generated MSW is being dumped in improper landfills, accrediting MSW as the 4th largest source of global emission and the 3rd largest source of methane emission [3,4]. On the other hand, over exploitation of fossil fuels to meet energy demand is causing serious environmental issues

as well. According to a report, the coal-based power plant will continue as the largest and important component to meet the world energy demand, and is expected to double in the first three decades of the 21st century [5]. Coal-fired power plants are cited as one of the major sources of environmental pollution in terms of the emission of Sox, CO<sub>x</sub>, NO<sub>x</sub>, particulate matter (PM), and heavy metals such as mercury, which get accumulated in water and air and lead to severe health hazards [6–9].

Most of the developing countries are attempting to achieve domestic energy security and minimize the environmental impact due to uncontrolled MSW. Similar to other developing countries, Pakistan is under an energy crisis and facing serious health and environmental threats due to mismanagement of MSW. At present, the annual generation of MSW is about 32.3 million tons of MSW. The treatment and disposal of MSW is a challenging task for municipalities in Pakistan, and even major cities rely on open dumping of generated MSW. Thus, it would be beneficial to find an alternative solution for utilizing the enormous amount of non-recycled MSW. From the environmental point of view, there are various strategies such as waste to products/waste to energy technologies (incineration, gasification, and pyrolysis), anaerobic digestion, and composting as an alternative to disposal of MSW in landfills. In light of current MSW collection practices in the country (single bin system), implementation of separate/sorting type of collection system for food waste at households is a currently dire need. In this way, nutrients of biowaste can be utilized as organic fertilizers, whereas the energy potential it contains may be utilized to produce biogas fuel. In addition to this, separation of biowaste from the main waste stream will cause a reduction in moisture and Cl content, enabling residual waste with improved heating value. Furthermore, high moisture content in MSW can lead to difficulty in the recycling process and can increase the production of leachate as well. The high moisture content and heterogeneous nature are the main issues linked with MSW as fuel. However, treatment/processing of MSW can lead to high quality waste derived fuels, such as solid recovered fuel (SRF) and refuse derived fuel (RDF) [10].

Incineration of waste derived fuels, especially RDF with high heating value, high degree volume reduction, and effective energy recovery, makes it an essential part of the waste to energy scheme. RDF usually contains combustible materials obtained from municipal solid wastes after implementation of a combination of unit operations such as sorting, mechanical separation, screening, and size reduction [11]. This makes RDF a better fuel with more predictable characteristics, including high calorific value and energy density, compared to the municipal solid waste. This alteration of MSW into RDF may show significant improvement in: (a) recovery of materials such as glass and metal which may be reused or recycled, (b) reduction in materials which can contribute to pollution and maintenance issues, and c) enhanced consistency of RDF may help to transport and market it as a commodity to solid fuel consumers [12].

Due to aspects such as the abundance of availability of coal and the long life of coal fired power plants, the usage of coal for power generation has been increased in developing countries. The co-combustion of coal and RDF could be a feasible approach that may be integrated with an already existing coal fired power plant scheme to supplement the reduction in consumption of coal and the costs of the main fuel. In addition to this, low level of sulfur and nitrogen content in waste derived fuel may improve the environmental performance (i.e., NO<sub>x</sub>, SO<sub>x</sub>, and CO<sub>2</sub> emissions) of coal power plants [13,14]. However, the environmental concern about pollutants such as dioxins, HCl, furans, and other unburned hydrocarbon has received a lot of attention. In addition to environment issues, the higher chlorine and alkaline content in waste fuels may contribute to corrosion and ash deposition issues in waste to energy plants [2,15]. Various investigations and surveys have indicated that co-combustion of RDF with coal can benefit in many ways, such as: (a) reduction in greenhouse gases (GHG) and leachate from the landfill source [16,17], (b) formation of corrosive deposits in the boiler during sole combustion of RDF can be reduced with co-combustion strategy [18], and (c) the higher volatile content of RDF lowers the ignition temperature of lignite coal and facilitates early combustion [19].

Co-combustion of solid waste fuels derived from the non-hazardous waste sources has the capacity of covering a substantial part of the future demand of energy by keeping an eye on economic and environmental benefits. In this work, thermogravimetric analysis was carried out to find co-combustion thermal characteristics and kinetic parameters of RDF with low-rank local coal by using model-free methods. In fact, it intends to explain possible synergistic phenomena involved during the co-combustion of these fuels. In this way, an additional value of this work is demonstrated by the choice of fuel in terms of local availability and future sustainability. This study emphasizes the co-firing of low-rank local coal and RDF as a resource to reduce the amount of solid wastes to landfill, by utilizing it under the waste to energy strategy.

## 2. Materials and Methods

The co-combustion experiments of RDF and low-rank coal were performed using the Mettler Toledo thermogravimetry (TG-DTG) system. The coal sample used in this research was taken from a Chiragh source in Pakistan, whereas true simulated RDF samples, including four major waste fractions: textile (37.6%), paper (13.3%), nylon plastic (47.3%), and PET (1.8%), were prepared based on the detailed physical characterization of MSW in the city of Lahore, Pakistan as described in our previous work [20]. The basic characterization work related to individual fractions of RDF and coal, such as proximate and ultimate analysis (Table 1), environmental issues (heavy metal content and leaching), energy potential, and thermal properties has been presented in our last work [21].

**Table 1.** Proximate & ultimate analysis of selected samples [20,21].

Samples	Proximate Analysis <sup>ad</sup>					Ultimate Analysis <sup>daf</sup>				
	H <sub>2</sub> O (%)	VM (%)	Ash (%)	FC <sup>d</sup> (%)	C (%)	H (%)	O <sup>d</sup> (%)	N (%)	S (%)	HHV (kJ/kg)
Textile	2.94	81.23	5.01	10.82	58.4	4.98	35.7	0.6	0.16	20,392
Nylon plastic bags	0.02	93.71	5.52	0.741	78.7	12.4	8.7	0.12	0.02	40,416
Paper	3.44	75.85	18.82	1.89	50.5	6.41	42.3	0.22	0.55	16,239
PET bottles	ND	92.26	0.19	7.55	62.0	4.04	33.9	0.05	0.01	23,060
RDF	1.6	86.2	7.07	4.7	66.9	8.7	23.8	0.32	0.14	29,429
Coal	1.84	38.8	31.7	27.53	80.7	3.6	9.6	1.02	5.04	30,362

<sup>ad</sup> air-dried basis, <sup>daf</sup> dried ash-free basis, and <sup>d</sup> calculated by difference.

In order to examine the effect of blending ration (co-firing of RDF and coal) on the thermal properties, RDF samples were added to selected coal samples to formulate the weight ratios of 10, 20, 30, and 40 by weight percent. The co-combustion experiments were performed with an initial sample size of ~20 mg, whereas a constant synthetic air flow rate of 80 mL/min was provided during all co-combustion experiments. Considering the complexity issue linked with true representation of various components of RDF and coal samples during thermal analysis in micro TGA, double milling action in nitrogen atmosphere was carried out to gain size reduction of ~200 µm. All TGA runs were conducted in the temperature range 25 °C to 1000 °C at four heating rates as 10, 20, 30, and 40 °C/min. Temperature profiles were programmed with a holding time of 10 and 30 min at temperatures of 105 °C and 1000 °C, respectively.

## 3. Kinetic Modelling

The level of complexity and composition diversity of the selected samples, particularly RDF, make it difficult to understand the involved phenomena. Although thermal analyses give some indication about kinetics during thermal decomposition, combustion remains a complex process that includes various mechanisms. The research community has mainly developed two approaches known as model-fitted and isoconversional (model-free), to explain the impact of different operating parameters, and to notice all the possible interactions during the combustion process. These methods describe the conversion process by

determination of kinetic parameters from TGA results [22]. At present, the literature review about determination of kinetic parameters recommends that isoconversional (model-free) methods are significantly more accurate and reliable when compared to the model-fitting methods, as the model-fitting approach always has a possibility of error in picking an appropriate reaction model [23–26], whereas isoconversional methods do not possess any pre-assumption regarding reaction mechanism. This ultimately leads to more accurate and precise kinetic data for homogeneous and heterogeneous combustion processes with a requirement of a series of measurements at different heating rates. Keeping this in mind, two of the main isoconversional methods, Kissinger–Akahira–Sunose (KAS) and Flynn–Wall–Ozawa (FWO), were applied to determine the kinetic parameters for the co-combustion of coal and RDF.

The rate of reaction for solid fuel is written as:

$$\frac{d\alpha}{dt} = f(T) \times f(\alpha) \quad (1)$$

where:

$$f(T) = A \exp^{-\frac{E}{RT}} \quad (2)$$

In Equation (2)  $E$  (kJ/mol) is the activation energy,  $A$  is the pre-exponential ( $\text{min}^{-1}$ ) factor,  $R$  is the gas constant, and  $T$  is the absolute temperature (K). In Equation (1),  $\alpha$  is called fractional conversion, and for the thermal decomposition description of the samples it is given as:

$$\alpha = \frac{m_O - m_i}{m_O - m_\infty} \quad (3)$$

and  $f(\alpha)$  is a function of fractional conversion ( $\alpha$ ). Under constant temperature ramp conditions, Equation (1) can be converted into following form by using Equation (2):

$$\frac{d\alpha}{dT} = \frac{A}{\beta} \exp^{-\frac{E}{RT}} f(\alpha) \quad (4)$$

Equation (4) assumes that kinetic parameters such as  $E$ ,  $A$ , and  $f(\alpha)$  describe the time evolution of a physical and chemical change. Integration of Equation (4) gives:

$$g(\alpha) = \int_0^\alpha \frac{d\alpha}{f(\alpha)} = \frac{A}{\beta} \int_{T_0}^T \exp\left(-\frac{E}{RT}\right) dT = \left(\frac{AE}{\beta R}\right) p\left(\frac{E}{RT}\right) \quad (5)$$

where  $g(\alpha)$  is the integral form of the reaction model,  $T_0$  is the initial temperature, and  $p\left(\frac{E}{RT}\right)$  is the temperature integral, which does not have any analytical solution. Equation (5) can be further integrated as:

$$\ln g(\alpha) = \ln\left(\frac{AE}{R}\right) - \ln \beta + \ln p\left(\frac{E}{RT}\right) \quad (6)$$

### 3.1. Kissinger–Akahira–Sunose Method (KAS)

The KAS method is based on approximation of the Coats–Redfern method as shown in Equation (7):

$$p\left(\frac{E}{RT}\right) \cong \frac{\exp\left(-\frac{E}{RT}\right)}{\left(\frac{E}{RT}\right)^2} \quad (7)$$

By equative Equations (4) and (5), the KAS equation can be thus defined as:

$$\ln \frac{\beta}{T^2} = \ln\left(\frac{AR}{Eg(\alpha)}\right) - \frac{E}{RT} \quad (8)$$

The plot of  $\ln \frac{\beta}{T^2}$  vs.  $1/T$  for constant value of  $\alpha$  will result a straight line. The value of  $E$  can be obtained by the gradient of the curve which is signified by  $-\frac{E}{R}$ . This model has been used and found satisfactory by other researchers [27–29].

### 3.2. Flynn–Wall–Ozawa Method (FWO)

Ozawa, Flynn, and Wall independently suggested an isoconversional integral method and calculated the temperature integral value in Equation (5) by using Doyle's approximation which leads to Equation (6).

$$\ln(\beta) = \ln\left[\frac{AE}{Rg(\alpha)}\right] - 5.331 - 1.052 \frac{E}{RT} \quad (9)$$

This equation is known as the OFW isoconversional model. Thus, for  $\alpha = const.$ , the plot of the left-hand side of Equation (9) vs.  $1/T$ , obtained from TGA curves at various heating rates, yields straight lines for different conversions. The  $E$  is determined from the slopes of these lines. This model has been used by many researchers [30,31].

## 4. Results and Discussion

### 4.1. Thermal Decomposition

The obtained TG (% weight loss) and DTG (rate of weight loss) thermograms for low-rank coal, RDF, and coal/RDF blends (10%, 20%, 30%, and 40% of RDF in coal) at a heating rate 10 °C/min under air atmosphere are illustrated in Figures 1 and 2. Generally, for solid fuels, thermograms consist of three regions which are linked with: (a) release of moisture content, (b) release of low and high volatile organic content, and (c) combustion of fixed carbon in fuel [32]. These obtained profiles show that weight loss in first and third regions was less prominent, as all samples contained very low moisture and fixed carbon. In contrast to coal, RDF displays diverse behavior of weight loss, as it is heterogenous in nature and comprises of various fuel constituents. It is evident from DTG profiles of RDF and coal that, due to the high reactivity of RDF, quick weight loss is observed via two prominent peaks, compared to a single peak of coal which is attributed to release of carbon containing volatile matter [33,34]. The slow release of volatile matter in coal shows that coal requires a higher temperature to initiate the combustion process. For coal at a heating rate of 10 °C/min, the maximum weight loss rate of 0.1 (%/S) is observed at peak temperatures of 555 °C. In the case of RDF, the first peak shows a maximum weight loss rate of 0.147 (%/S) at a peak temperature of 341 °C, representing easy decomposition of highly volatile components such as paper and textile. The second peak shows a maximum weight loss rate of 0.11 (%/S) at a peak temperature of 465 °C, mainly contributed to the decomposition of thermally stable mixed plastic (LDPE, HDPE, and PVC) [35,36].

Table 2 presents the combustion characteristics such as ignition temperature ( $T_i$ ), burnout temperature ( $T_f$ ), the combustion residue mass ( $M_f$ ), the temperature at maximum weight loss rate of the first peak and the second peak ( $T_1$  and  $T_2$ ), and the mass loss rate for first and second peak ( $DTG_1$  and  $DTG_2$ ). As ignition and burnout temperatures of fuels are key parameters to evaluate fuel selection, combustion design, and safe transportation and storage [37], intersection and conversion methods were employed for the investigation of ignition and burnout temperatures [38].

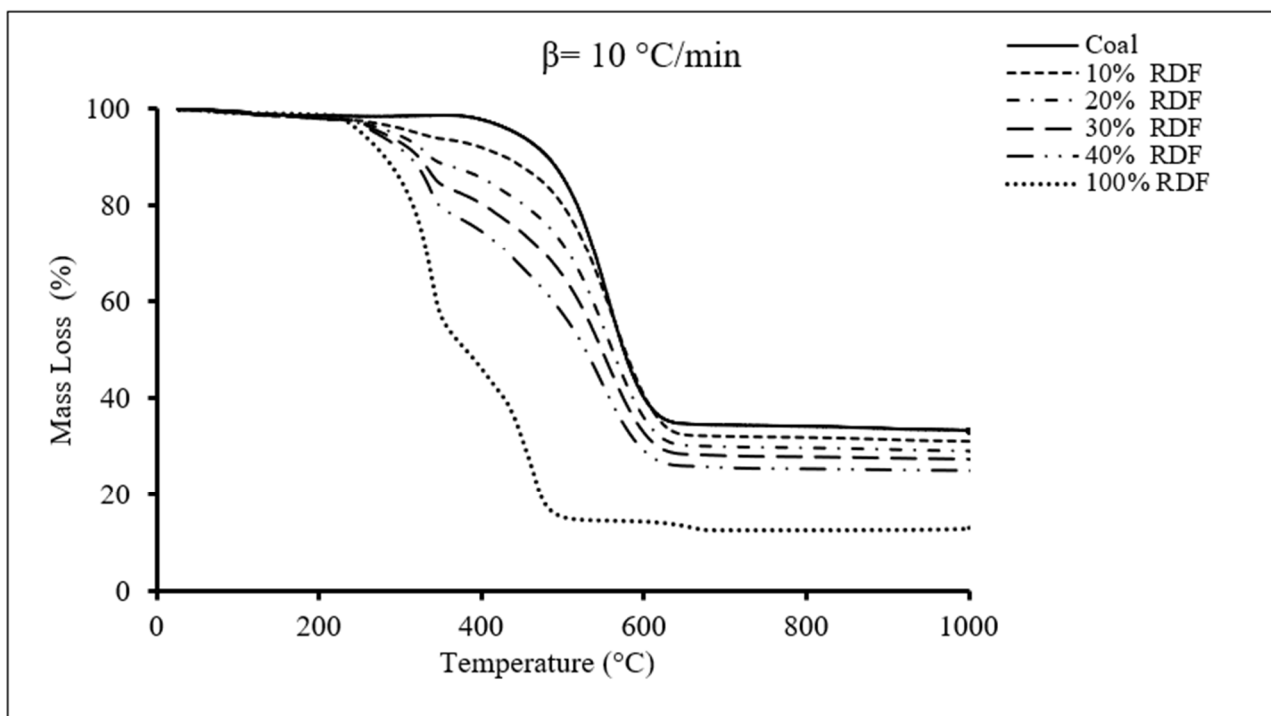


Figure 1. TGA profiles of coal, RDF, and coal/RDF blends for combustion process.

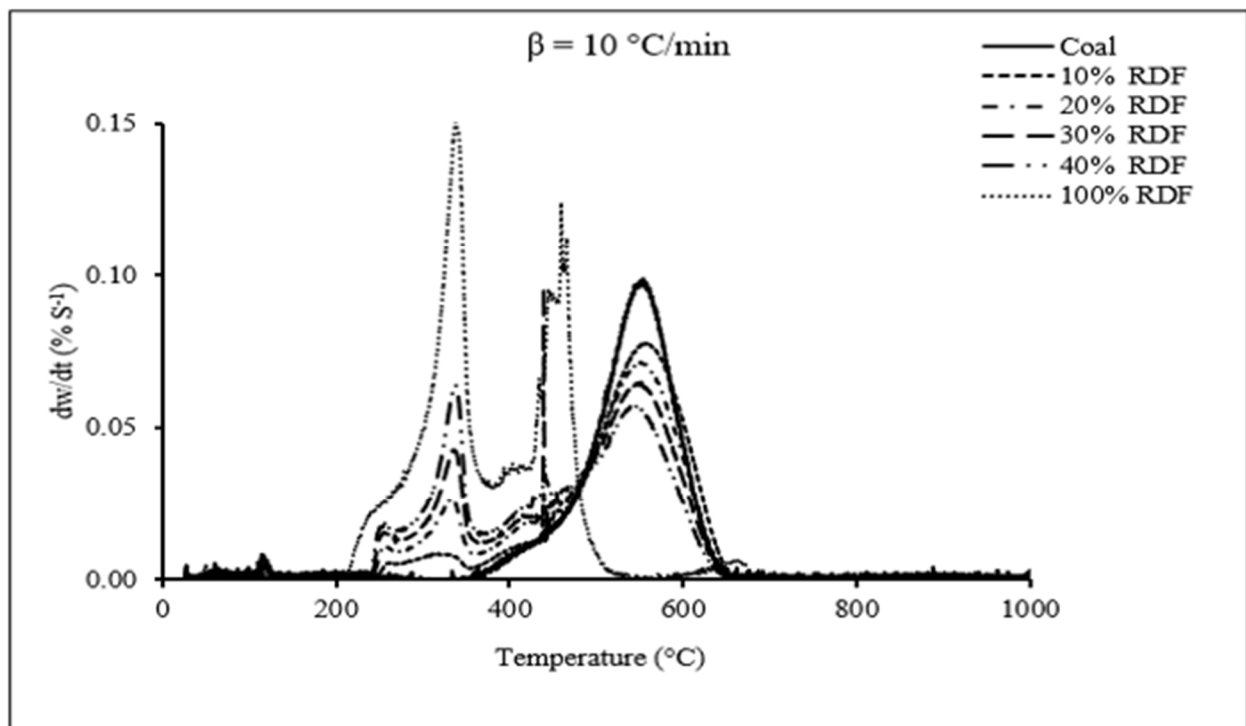


Figure 2. DTG profiles for coal, RDF, and coal/RDF blends for combustion process.

**Table 2.** The co-combustion characteristics parameters of coal, RDF, and their blends at heating rate 10 °C/min.

Sample	$T_i$ (°C)	$T_f$ (°C)	$M_f$ (%)	$T_1$ (°C)	$T_2$ (°C)	$DTG1$ (%/s)	$DTG2$ (%/s)
Coal and RDF blends							
100% Coal	460	620	32.9	561	-	0.10	-
90% Coal + 10% RDF	423	618	31.3	340	567	0.01	0.08
80% Coal + 20% RDF	390	626	28.7	347	559	0.02	0.07
70% Coal + 30% RDF	340	610	27.1	350	547	0.04	0.06
60% Coal + 40% RDF	298	608	24.8	351	536	0.06	0.05
100% RDF	280	474	13	341	465	0.14	0.12

$T_i$ : the ignition temperature;  $T_f$ : burnout temperature;  $M_f$ : the combustion residue mass;  $T_1, T_2$ : temperature at maximum weight loss rate of first peak and second peak;  $DTG1$ : the mass loss rate for first peak; and  $DTG2$ : the mass loss rate for second peak.

Generally, ignition temperature is associated with the temperature at which devolatilization starts. Mostly, devolatilization of carbonaceous matter in waste derived fuels occurs at temperatures lower than the temperature at which devolatilization of coal takes place [39]. The ignition temperature of the RDF and coal samples occurs at 280 °C and 460 °C, respectively. The burnout and peak temperatures for coal occurred at a much higher temperature zone than RDF. The burnout temperature of RDF and coal samples reaches 474 °C and 620 °C, respectively. This means that combustion of RDF is taking place earlier and easier than that of coal. It is noticeable that the lower ash content in the RDF sample is facilitating the diffusion of oxygen to the surface of char, rather than limiting the reactivity by hindering the diffusion, as in case of coal [40]. The thermal assessment profiles and trends of co-combustion coal/RDF blends are in good accord with other authors' findings [2,10,41].

#### 4.2. Effect of Blending of Coal with RDF

The interactive effect of co-combustion of coal and RDF blends are represented in Figures 1 and 2. The co-combustion parameters from these TG-DTG profiles are represented in Table 2. These results show that the ignition temperature of low-rank coal decreases as the blending ratio of RDF increases in the blends. As the ratio of RDF is increased, behavior is more predisposed to RDF decomposition. This may be attributed to the early release of volatile content in RDF, resulting in quicker weight loss during combustion of the blends. Higher volatile content in the fuel may lead to easier ignition and early completion of the combustion process. This distinguishes the co-combustion behavior of coal/RDF blends compared to low-rank coal. As in the case of coal, the combustion is mainly linked with carbon-containing volatile matter and fixed carbon, whereas in the case of RDF, this is dominated by easily combustible volatile matter. Therefore, it is evident that the addition of high volatile RDF in coal will always lower the ignition temperature, due to the emission of volatile at a lower temperature. The lowest ignition temperature of 298 °C was obtained for the blend of 60% coal + 40% RDF. This reduction in ignition temperatures during co-combustion coal with RDF was observed by other authors as well [2,10,19,42]. Similarly, a minor improvement in the burnout temperature of coal/RDF blends was observed compared to low-rank coal. Furthermore, it is worth noting that the reduction in ash content shows a direct relation with the blending ratio. As the blending ratio increases, ash content decreases.

The DTG co-combustion profile (refer to Figure 2) shows that the reactivity of low-rank coal has been significantly improved with the increase in RDF in coal/RDF blends. It is evident that, with an increase in blending ratio, mass loss started at lower temperature zones due to an increase in volatile content. This means the release of the volatile content of the RDF produced enough energy to facilitate the early combustion of coal. Generally, it is considered that the reactivity is directly proportional to the height of the DTG peak,

and inversely proportional to peak temperature. In this investigation, all the results under co-combustion of coal and RDF show that RDF is more reactive than low-rank coal, and the increasing blending ratio of RDF will lead to lower ignition and burnout temperatures, in addition to low ash content benefits (refer to Table 2). Furthermore, owing to major changes in second peaks at higher blending ratios (refer to Figure 2), results indicate that synergistic effects exist during the co-combustion of coal and RDF [39,43].

#### 4.3. Kinetic Analyses

Owing to the existence of multiple components and their simultaneous and consecutive reactions, the kinetic analysis of solid fuels, particularly of RDF during a combustion phase, is extremely complex. In order to determine the effect of the blending ratio on the combustion characteristics of the blends, the two isoconversional methods, FWO and KAS, were used to measure the  $E$  of the coal and RDF blends at different conversion rates. The associated plots for these methods for conversion ( $\alpha$ ) range between 0.1 and 0.9, are shown in Figures 3 and 4. The parallelism of these lines is recognized by the same mechanism of the reaction and kinetic behavior. Most of the time, correlation coefficients determined by the FWO and KAS methods are close to unity, indicating that both methods are suitable for the estimation of  $E$  on micro TGA. For the said range of conversion, ( $\alpha$ ),  $E$ , and correlation coefficient ( $R^2$ ) values obtained from individual slopes based upon the liner model equation are summarized in Table 3.

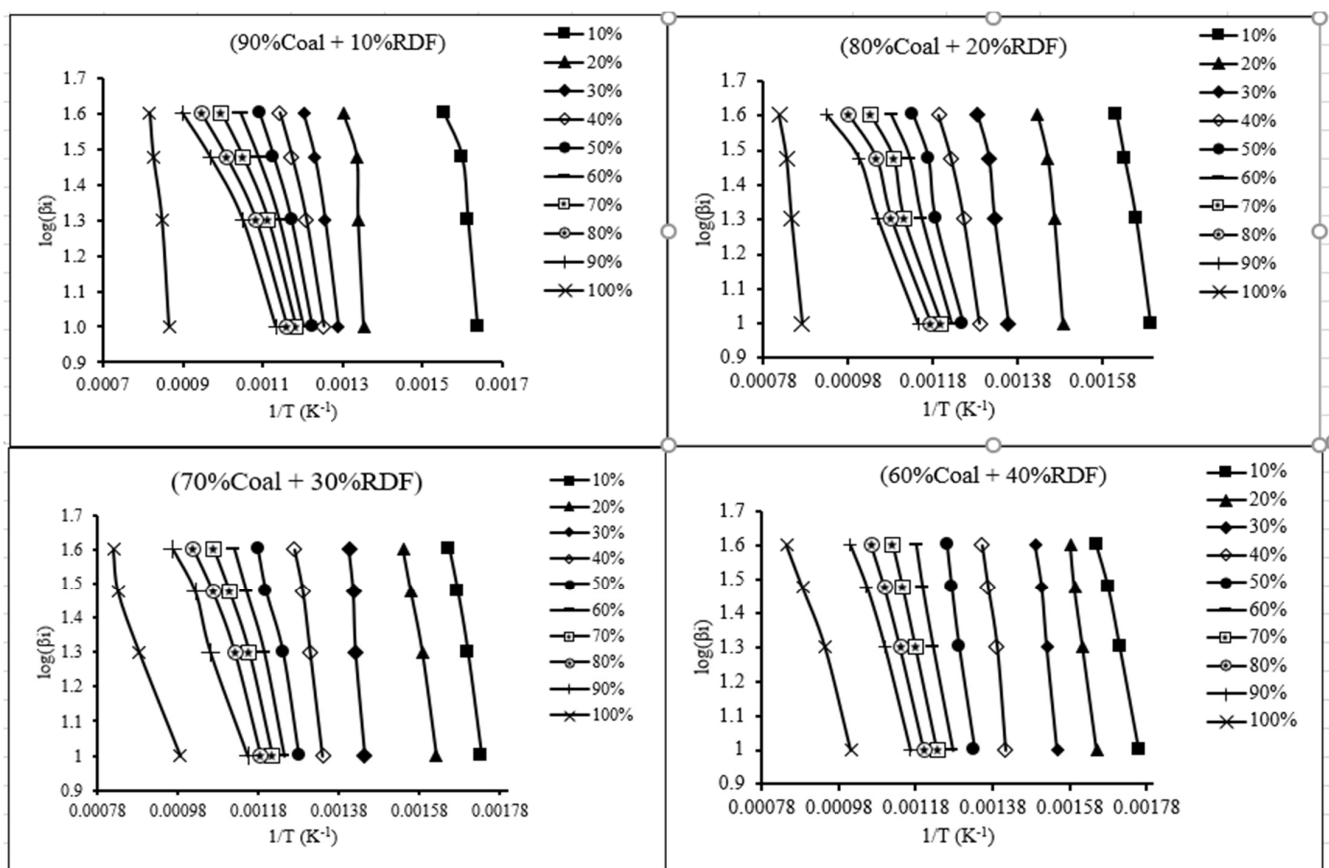


Figure 3. Plots for kinetic model, FWO for various blends of coal/RDF.

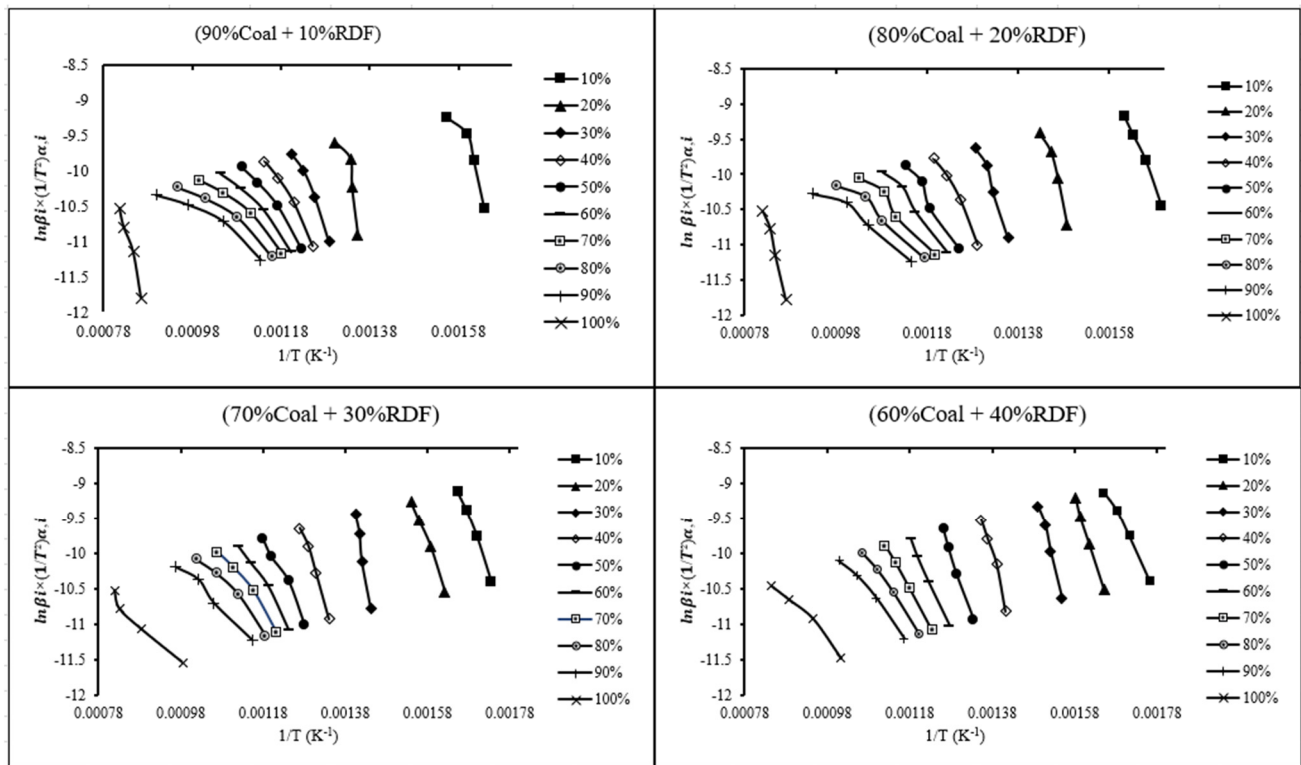


Figure 4. Plots for kinetic model, KAS for various blends of coal/RDF.

As both FWO and KAS are considered to be applicable for multiple-step reactions, as in this study, the changing trend of  $E$  values obtained by both models show similar trend, as shown in Figure 5. Clearly, different non-monotonic trends are obtained for all blending cases (Figure 5), indicating the complexity of the coal/RDF blends. An increase in RDF contents in the blend from 10% to 40% results in a significant rise in average  $E$  by ~43% and ~35%, determined by KAS and FWO, respectively (Table 3). This increasing tendency in the average values of  $E$  with the increase in RDF content strongly suggests that certain components of RDF are not favorable for weakening the reaction barrier of overall blending combustion. However, the flattening of steep (near to bell shaped) curves and shifting of peak  $E$  values towards higher  $\alpha$  with increasing RDF contents signify that coal combustion is the main barrier during early conversion stage. After the peak  $E$  value is reached, a more rapid decrease in  $E$  value is observed for higher coal blending compositions while, in comparison, higher RDF blend compositions show a less rapid decrease in  $E$  with the increasing  $\alpha$  value (Table 3 and Figure 5). Although, there is a shift in peak  $E$  position with changing blending compositions, no significant difference in the maximum  $E$  value is observed for most of the blending cases (Figure 5). Only the 70% coal + 30% RDF case shows a decrease in maximum  $E$  value. In all blending cases, after the maximum  $E$  is achieved, monotonicity in decreasing trends is observed, suggesting that once the reaction barrier is crossed, resultant products do not offer any significant negative impact on combustion (Figure 5).

**Table 3.** Kinetic parameters of combustion of coal, RDF, and coal/RDF blends.

Blending	90% Coal + 10% RDF				80% Coal + 20% RDF				70% Coal + 30% RDF				60% Coal + 40% RDF			
	KAS		FWO		KAS		FWO		KAS		FWO		KAS		FWO	
( $\alpha$ )	R <sup>2</sup>	E (kJ/mol)	R <sup>2</sup>	E (kJ/mol)	R <sup>2</sup>	E (kJ/mol)	R <sup>2</sup>	E (kJ/mol)	R <sup>2</sup>	E (kJ/mol)	R <sup>2</sup>	E (kJ/mol)	R <sup>2</sup>	E (kJ/mol)	R <sup>2</sup>	E (kJ/mol)
0.1	0.827	118.9	0.85	123	0.992	129.2	0.993	132.5	0.992	133.2	0.993	136	0.992	94.7	0.993	99.3
0.2	0.7198	183.8	0.745	186.7	0.934	182	0.941	184	0.992	128.6	0.993	132.3	0.996	155.8	0.997	158
0.3	0.967	122.3	0.974	129	0.966	152.4	0.971	156.9	0.982	160.3	0.984	165	0.988	189.5	0.99	190.7
0.4	0.98	90.4	0.985	99.15	0.973	106.6	0.979	114.1	0.987	151.3	0.989	156	0.974	176.7	0.977	179.5
0.5	0.979	71.74	0.986	81.9	0.974	86.3	0.98	95.3	0.979	96.14	0.984	104.3	0.995	147.7	0.995	152.6
0.6	0.971	57.37	0.983	68.7	0.982	69.7	0.998	80.1	0.984	79.1	0.989	88.6	0.998	109.8	0.998	117.2
0.7	0.96	46.2	0.979	58.5	0.968	56.5	0.98	67.8	0.979	65.1	0.987	75.8	1	86.8	1	96
0.8	0.947	38	0.975	51.1	0.964	46.2	0.981	58.6	0.971	53.7	0.983	65.4	0.995	69.9	0.997	80.4
0.9	0.93	32.24	0.972	46.3	0.947	38.8	0.976	52.1	0.981	47.7	0.991	60.2	0.984	58.6	0.991	70.3
Average		97		106		108		116		95		103		114		121

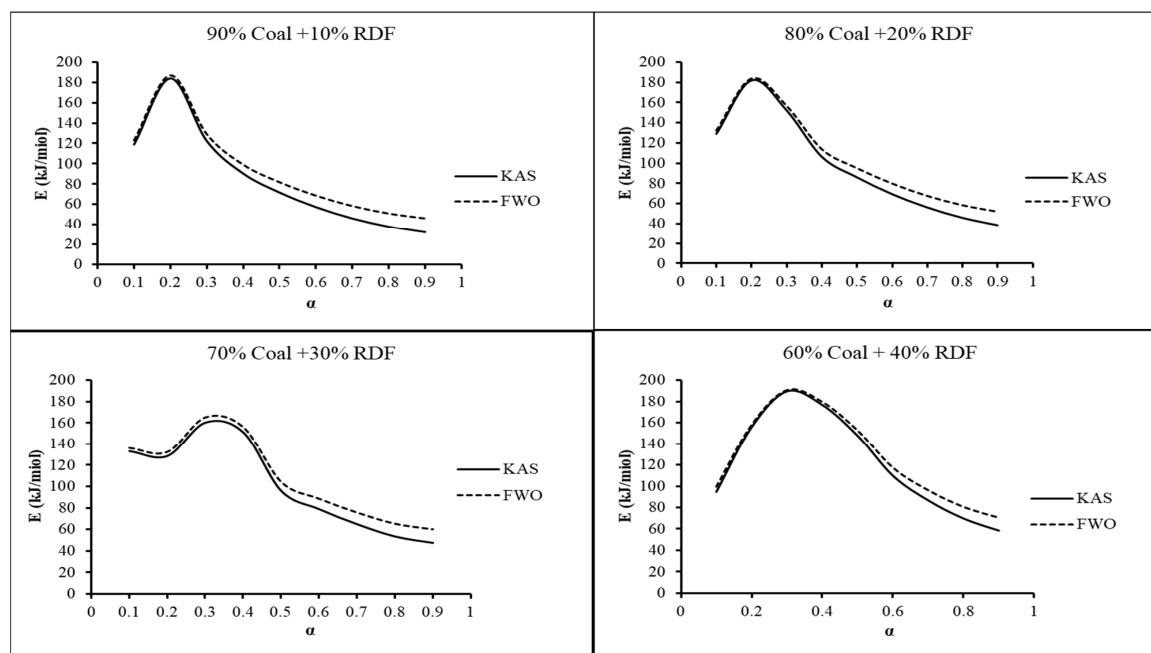


Figure 5. Relationship between  $E$  and  $\alpha$  for coal and RDF blends by KAS and FWO methods.

## 5. Conclusions

This study sought to explore the co-combustion characteristics and kinetic analyses of low-quality coal, RDF, and their blends under different heating rates by the TGA method. According to TG and DTG curves, when comparing the combustion characteristics of coal, RDF, and their blends to coal alone, the blends performed better, as RDF blending improves the ignition temperature and devolatilization of low-rank coal. Furthermore, blending RDF improves the reactivity of low-reactive char combustibles, lowering the amount of unburned fuel. An increase in RDF contents in the blend from 10% to 40% results in the lowest ignition temperature of 298 °C and a significant rise in average  $E$  by ~43% and ~35%, determined by KAS and FWO, respectively. The coal/RDF blend with 70%/30% ratio had the lowest average activation energy of all the blends, suggesting it to be the best possible option for co-combustion.

The TGA employs 20 mg of material for the thermal kinetic tests, and application of these results to a commercial co-combustion facility would involve a scale-up by many orders of magnitude. Future work can include scale-up of the co-combustion to gram and kilogram quantities at lab and pilot-scales.

**Author Contributions:** Conceptualization, M.A. and S.S.J.; methodology, M.A., S.S.J.; software, A.A., F.W. (Florian Wesenauer); validation, M.A., A.A. and F.W. (Florian Wesenauer); formal analysis, M.A., S.S.J. and C.J.; investigation, S.M., N.R.; resources, M.A., S.M., N.R.; data curation, F.W. (Florian Wesenauer), M.A.; writing—original draft preparation, M.A.; writing—review and editing, M.A., S.M.; visualization, F.W. (Franz Winter), C.J.; supervision, F.W. (Franz Winter), M.H.; project administration, F.W. (Franz Winter), M.H.; funding acquisition, F.W. (Franz Winter), M.H. All authors have read and agreed to the published version of the manuscript.

**Funding:** This research received no external funding.

**Institutional Review Board Statement:** Not applicable.

**Informed Consent Statement:** Not applicable.

**Acknowledgments:** The authors thank the Austrian Research Promotion Agency (FFG) for its financial support through project number (876737) and University of the Punjab, Lahore, Pakistan

for Ph.D. scholarship. The authors also acknowledge the TU-Wien University Library for financial support through its Open Access Funding Program.

**Conflicts of Interest:** The authors declare no conflict of interest.

### Nomenclature

TGA	Thermogravimetric Analysis
MC	Moisture Content
FC	Fixed Carbon
RDF	Refuse Derived Fuel
HHV	High Heating Value
VM	Volatile Matter
MSW	Municipal Solid Waste
ad	air-dried basis
daf	dried ash-free basis
$\alpha$	Fractional Conversion
$E_{\alpha}$	Activation Energy (kJ/mol)
A	Pre-exponential Factor
$\beta$	Heating Rate ( $^{\circ}\text{C}/\text{min}$ )
R	General Gas Constant
$f(\alpha)$	Differential Form of Reaction Model
$g(\alpha)$	Integral Form of Reaction Model
$R^2$	Correlation Co-efficient

### References

- Lee, Z.H.; Sethupathi, S.; Lee, K.T.; Bhatia, S.; Mohamed, A.R. An overview on global warming in Southeast Asia: CO<sub>2</sub> emission status, efforts done, and barriers. *Renew. Sustain. Energy Rev.* **2013**, *28*, 71–81. [[CrossRef](#)]
- Isaac, K.; Bada, S.O. The co-combustion performance and reaction kinetics of refuse derived fuels with South African high ash coal. *Heliyon* **2020**, *6*, e03309. [[CrossRef](#)] [[PubMed](#)]
- Zuberi, M.J.S.; Ali, S.F. Greenhouse effect reduction by recovering energy from waste landfills in Pakistan. *Renew. Sustain. Energy Rev.* **2015**, *44*, 117–131. [[CrossRef](#)]
- Matthews, E.; Themelis, N. Potential for reducing global methane emissions from landfills, 2000–2030. In Proceedings of the Eleventh International Waste Management and Landfill Symposium, Cagliari, Italy, 1 October 2007.
- Sajwan, K.S.; Alva, A.K.; Punshon, T.; Twardowska, I. *Coal Combustion Byproducts and Environmental Issues*; Springer: Berlin/Heidelberg, Germany, 2006; Volume 81.
- Munawer, M.E. Human health and environmental impacts of coal combustion and post-combustion wastes. *J. Sustain. Min.* **2018**, *17*, 87–96. [[CrossRef](#)]
- Srivastava, R.K.; Hall, R.E.; Khan, S.; Culligan, K.; Lani, B.W. Nitrogen oxides emission control options for coal-fired electric utility boilers. *J. Air Waste Manag. Assoc.* **2005**, *55*, 1367–1388. [[CrossRef](#)] [[PubMed](#)]
- Srivastava, R.K.; Jozewicz, W.; Singer, C. SO<sub>2</sub> scrubbing technologies: A review. *Environ. Prog.* **2001**, *20*, 219–228. [[CrossRef](#)]
- Granite, E.J.; Pennline, H.W.; Senior, C. *Mercury Control: For Coal-Derived Gas Streams*; John Wiley & Sons: Hoboken, NJ, USA, 2015.
- Chang, Y.-H.; Chen, W.; Chang, N.B. Comparative evaluation of RDF and MSW incineration. *J. Hazardous Mater.* **1998**, *58*, 33–45. [[CrossRef](#)]
- Çepelioğullar, Ö.; Haykırı-Açma, H.; Yaman, S. Kinetic modelling of RDF pyrolysis: Model-fitting and model-free approaches. *Waste Manag.* **2016**, *48*, 275–284. [[CrossRef](#)] [[PubMed](#)]
- Reza, B.; Soltani, A.; Ruparathna, R.; Sadiq, R.; Hewage, K. Environmental and economic aspects of production and utilization of RDF as alternative fuel in cement plants: A case study of Metro Vancouver Waste Management. *Resour. Conserv. Recycl.* **2013**, *81*, 105–114. [[CrossRef](#)]
- Malat'ák, J.; Velebil, J.; Bradna, J. Specialty types of waste paper as an energetic commodity. *Agron. Res.* **2018**, *16*, 534–542.
- Yanik, J.; Duman, G.; Karlström, O.; Brink, A. NO and SO<sub>2</sub> emissions from combustion of raw and torrefied biomasses and their blends with lignite. *J. Environ. Manag.* **2018**, *227*, 155–161. [[CrossRef](#)] [[PubMed](#)]
- Vekemans, O.; Chaouki, J. Municipal solid waste Co-firing in coal power plants: Combustion performance. *Dev. Combust. Technol.* **2016**, 118–142. [[CrossRef](#)]
- Zhang, S.; Lin, X.; Chen, Z.; Li, X.; Jiang, X.; Yan, J. Influence on gaseous pollutants emissions and fly ash characteristics from co-combustion of municipal solid waste and coal by a drop tube furnace. *Waste Manag.* **2018**, *81*, 33–40. [[CrossRef](#)] [[PubMed](#)]
- Chen, X.; Xie, J.; Mei, S.; He, F. NO<sub>x</sub> and SO<sub>2</sub> Emissions during Co-Combustion of RDF and Anthracite in the Environment of Precalciner. *Energies* **2018**, *11*, 337. [[CrossRef](#)]

18. Zabetta, E.C.; Barišić, V.; Peltola, K.; Hotta, A. Foster Wheeler Experience with biomass and waste in CFBs. In Proceedings of the 33rd International Technical Conference on Coal Utilization and Fuel Systems, Clearwater, FL, USA, 1–5 June 2008.
19. Iordanidis, A.; Asvesta, A.; Vasileiadou, A. Combustion behaviour of different types of solid wastes and their blends with lignite. *Therm. Sci.* **2018**, *22*, 1077–1088. [[CrossRef](#)]
20. Azam, M.; Jahromy, S.S.; Raza, W.; Raza, N.; Lee, S.S.; Kim, K.-H.; Winter, F. Status, characterization, and potential utilization of municipal solid waste as renewable energy source: Lahore case study in Pakistan. *Environ. Int.* **2020**, *134*, 105291. [[CrossRef](#)] [[PubMed](#)]
21. Azam, M.; Jahromy, S.S.; Raza, W.; Jordan, C.; Harasek, M.; Winter, F. Comparison of the combustion characteristics and kinetic study of coal, municipal solid waste, and refuse-derived fuel: Model-fitting methods. *Energy Sci. Eng.* **2019**, *7*, 2646–2657. [[CrossRef](#)]
22. Boumanchar, I.; Chhiti, Y.; Alaoui, F.E.M.h.; Elkhouchi, M.; Sahibed-Dine, A.; Bentiss, F.; Jama, C.; Bensitel, M. Investigation of (co)-combustion kinetics of biomass, coal and municipal solid wastes. *Waste Manag.* **2019**, *97*, 10–18. [[CrossRef](#)] [[PubMed](#)]
23. Burnham, A.K.; Dinh, L. A comparison of isoconversional and model-fitting approaches to kinetic parameter estimation and application predictions. *J. Therm. Anal. Calorim.* **2007**, *89*, 479–490. [[CrossRef](#)]
24. Burnham, A.K. How to Model Maturation and Pyrolysis. In *Global Chemical Kinetics of Fossil Fuels*; Springer International Publishing: New York, NY, USA, 2017.
25. White, J.E.; Catallo, W.J.; Legendre, B.L. Biomass pyrolysis kinetics: A comparative critical review with relevant agricultural residue case studies. *J. Anal. Appl. Pyrolysis* **2011**, *91*, 1–33. [[CrossRef](#)]
26. Vyazovkin, S.; Burnham, A.K.; Criado, J.M.; Pérez-Maqueda, L.A.; Popescu, C.; Sbirrazzuoli, N. ICTAC Kinetics Committee recommendations for performing kinetic computations on thermal analysis data. *Thermochim. Acta* **2011**, *520*, 1–19. [[CrossRef](#)]
27. Ceylan, S.; Topçu, Y. Pyrolysis kinetics of hazelnut husk using thermogravimetric analysis. *Bioresour. Technol.* **2014**, *156*, 182–188. [[CrossRef](#)]
28. Mishra, G.; Bhaskar, T. Non isothermal model free kinetics for pyrolysis of rice straw. *Bioresour. Technol.* **2014**, *169*, 614–621. [[CrossRef](#)] [[PubMed](#)]
29. Ma, Z.; Wang, J.; Yang, Y.; Zhang, Y.; Zhao, C.; Yu, Y.; Wang, S. Comparison of the thermal degradation behaviors and kinetics of palm oil waste under nitrogen and air atmosphere in TGA-FTIR with a complementary use of model-free and model-fitting approaches. *J. Anal. Appl. Pyrolysis* **2018**, *134*, 12–24. [[CrossRef](#)]
30. Budrugaec, P.; Homentcovschi, D.; Segal, E. Critical analysis of the isoconversional methods for evaluating the activation energy. I. Theoretical background. *J. Therm. Anal. Calorim.* **2000**, *63*, 457–463. [[CrossRef](#)]
31. Šimon, P. Isoconversional methods. *J. Therm. Anal. Calorim.* **2004**, *76*, 123. [[CrossRef](#)]
32. Özsin, G.; Pütün, A.E. Kinetics and evolved gas analysis for pyrolysis of food processing wastes using TGA/MS/FT-IR. *Waste Manag.* **2017**, *64*, 315–326. [[CrossRef](#)] [[PubMed](#)]
33. Idris, S.S.; Abd Rahman, N.; Ismail, K.; Alias, A.B.; Abd Rashid, Z.; Aris, M.J. Investigation on thermochemical behaviour of low rank Malaysian coal, oil palm biomass and their blends during pyrolysis via thermogravimetric analysis (TGA). *Bioresour. Technol.* **2010**, *101*, 4584–4592. [[CrossRef](#)] [[PubMed](#)]
34. Muthuraman, M.; Namioka, T.; Yoshikawa, K. A comparison of co-combustion characteristics of coal with wood and hydrothermally treated municipal solid waste. *Bioresour. Technol.* **2010**, *101*, 2477–2482. [[CrossRef](#)] [[PubMed](#)]
35. Grammelis, P.; Basinas, P.; Malliopoulou, A.; Sakellariopoulos, G. Pyrolysis kinetics and combustion characteristics of waste recovered fuels. *Fuel* **2009**, *88*, 195–205. [[CrossRef](#)]
36. Sørum, L.; Grønli, M.; Hustad, J. Pyrolysis characteristics and kinetics of municipal solid wastes. *Fuel* **2001**, *80*, 1217–1227. [[CrossRef](#)]
37. Du, S.-W.; Chen, W.-H.; Lucas, J.A. Pretreatment of biomass by torrefaction and carbonization for coal blend used in pulverized coal injection. *Bioresour. Technol.* **2014**, *161*, 333–339. [[CrossRef](#)] [[PubMed](#)]
38. Lu, J.-J.; Chen, W.-H. Investigation on the ignition and burnout temperatures of bamboo and sugarcane bagasse by thermogravimetric analysis. *Appl. Energy* **2015**, *160*, 49–57. [[CrossRef](#)]
39. Wu, T.; Gong, M.; Lester, E.; Hall, P. Characteristics and synergistic effects of co-firing of coal and carbonaceous wastes. *Fuel* **2013**, *104*, 194–200. [[CrossRef](#)]
40. Cardozo, E.; Erlich, C.; Alejo, L.; Fransson, T.H. Combustion of agricultural residues: An experimental study for small-scale applications. *Fuel* **2014**, *115*, 778–787. [[CrossRef](#)]
41. Sezer, S.; Kartal, F.; Özveren, U. The investigation of co-combustion process for synergistic effects using thermogravimetric and kinetic analysis with combustion index. *Therm. Sci. Eng. Prog.* **2021**, *23*, 100889. [[CrossRef](#)]
42. Seo, M.W.; Kim, S.D.; Lee, S.H.; Lee, J.G. Pyrolysis characteristics of coal and RDF blends in non-isothermal and isothermal conditions. *J. Anal. Appl. Pyrolysis* **2010**, *88*, 160–167. [[CrossRef](#)]
43. Hu, S.; Ma, X.; Lin, Y.; Yu, Z.; Fang, S. Thermogravimetric analysis of the co-combustion of paper mill sludge and municipal solid waste. *Energy Convers. Manag.* **2015**, *99*, 112–118. [[CrossRef](#)]